

# Size-Inverse Molecular Sieving Xenon/Krypton Separation through Cation-Tuned Gating Effect within Linde Type A Zeolites

Corresponding Author: Professor Banglin Chen

This file contains all reviewer reports in order by version, followed by all author rebuttals in order by version.

Version 0:

Reviewer comments:

Reviewer #1

(Remarks to the Author)

The manuscript entitled “Size-Inverse Molecular Sieving Xenon/Krypton Separation through Cation-Tuned Gating Effect within Linde Type A Zeolites” presents the development of  $\text{Ag}^+$  and  $\text{Ca}^{2+}$  ion-exchanged LTA zeolites for Xe/Kr separation via a cation-tuned gating mechanism. The authors report a high IAST selectivity ( $>1600$ ) for Ag-LTA and a dynamic selectivity of 30 for  $\text{Ag}_9\text{Ca}_{1.5}\text{A}$ , supported by adsorption measurements, synchrotron PXRD, XAS, and DFT calculations. While the technical execution is strong, the manuscript does not meet the novelty and impact criteria for Nature Communications, for the following reasons:

1. Limited Conceptual Novelty

The cation-tuned gating (or “molecular trapdoor”) effect is well-established in the zeolite literature (e.g., Shang et al., JACS 2012; Lozinska et al., JACS 2012; Zhao et al., JACS 2021). The inversion from Kr-over-Xe to Xe-over-Kr selectivity via  $\text{Ag}^+$  exchange, while clearly demonstrated, constitutes a predictable extension of prior work rather than a fundamental advance. Silver-based zeolites for Xe capture have also been previously explored (Daniel et al., J. Phys. Chem. C 2013; Deliere et al., 2014).

2. Discrepancy Between Static and Dynamic Results

Despite the impressive static IAST selectivity, the  $\text{Ag}_{12}\text{A}$  material shows low Xe uptake in dynamic breakthrough tests, severely limiting practical relevance. While the authors address this by introducing  $\text{Ca}^{2+}$  to enhance sorption kinetics, the dynamic selectivity drops with increased Kr uptake, weakening the claim of “record performance.”

3. Overselling of Impact

Although the mechanism is well supported, the manuscript overstates the breakthrough significance of the work. Known limitations of Ag-zeolites such as silver leaching, long-term stability, and cost, are not adequately discussed or evaluated, which restricts the real-world applicability.

4. Incremental Improvement Over Prior Work

The tuning of cation density and mixed-cation strategies for gas separation are well-known techniques. The authors present a refined system, but not one that introduces a new material class or separation mechanism. The work thus falls short of the broader conceptual advances expected by Nature Communications.

In conclusion, this manuscript is well executed and presents a compelling mechanistic study of cation-gated Xe/Kr separation in LTA zeolites. However, the work represents an incremental advance rather than a transformative contribution, and the key claims are weakened by performance limitations under realistic conditions. Given these concerns, I do not recommend publication in Nature Communications. The manuscript may be better suited for a specialized journal in adsorption or materials chemistry.

Reviewer #2

(Remarks to the Author)

The manuscript titled “Size-Inverse Molecular Sieving Xenon/Krypton Separation through Cation-Tuned Gating Effect within Linde Type A Zeolites” presents a compelling conceptual and experimental advance in gas separation science. The authors develop a new paradigm for Xe/Kr separation using a cation-tuned gating mechanism in Linde Type A (LTA) zeolites, achieving a remarkable IAST selectivity of over 1600 and dynamic selectivity of 30. This is enabled by the selective interaction between Xe and  $\text{Ag}^+$  cations at key pore sites and is further optimized via partial substitution with  $\text{Ca}^{2+}$  to

alleviate kinetic limitations.

This work stands out for introducing an invertible molecular sieving mechanism, where the selective admission of the larger component (Xe) over the smaller one (Kr) is achieved through engineered gas–cation interactions rather than conventional size exclusion or equilibrium affinity alone. The authors combine adsorption isotherms, in situ synchrotron PXRD, breakthrough experiments, and DFT calculations to provide a thorough mechanistic explanation. Their approach not only redefines molecular sieving for noble gases but also suggests broader applicability to other challenging separations such as alkene/alkane mixtures.

Given the fundamental novelty, practical relevance, and excellent experimental and theoretical rigor, this is an outstanding and highly impactful piece of work. I strongly recommend minor revision prior to acceptance. The following comments are intended solely to clarify and strengthen the presentation, and do not detract from the scientific quality or significance of the findings. I look forward to seeing this work published following revision.

Some specific questions and suggestions for the authors' consideration:

1. The manuscript states that  $\text{Ag}^+$  and  $\text{Ca}^{2+}$  cannot be distinguished via diffraction in AgCa-LTA materials. However, it remains unclear which cation is primarily occupying the 8MR sites and acting as the door-keeping species. Since this directly affects the gating behavior, the authors should elaborate on any experimental trends (e.g., from synchrotron PXRD, EXAFS) or simulations (e.g., relative adsorption energies or stabilities) that may support a cation-specific site preference or functional role. Even a semi-quantitative trend would strengthen the mechanistic interpretation.
2. While the performance of Ag-LTA is impressive, several small-pore zeolites (e.g., CHA, KFI) are also known to exhibit molecular trapdoor effects. The authors should briefly justify the selection of LTA over other candidates. Is the framework geometry, cation accessibility, exchangeability, or known industrial usage the primary reason? A concise rationale would clarify the generalizability of this strategy.
3. The authors state that  $\text{Ag}_6\text{Ca}_3\text{A}$  shows measurable  $\text{N}_2$  uptake and BET surface area, implying a loss of cation-induced gating. Could the authors provide further insight into why the trapdoor mechanism collapses in this sample? Does  $\text{Ca}^{2+}$  incorporation exceed a critical threshold that weakens cation-framework interactions, displaces cations from 8MRs, or otherwise disrupts the gating configuration?
4. The manuscript introduces the term "size-inverse sieving" to describe preferential adsorption of the larger component (Xe). As this terminology may be unfamiliar to general readers, a clear definition early in the abstract or introduction would be helpful.
5. The manuscript refers to the threshold admission temperature using notations like "T<sub>ad</sub>" or "T<sub>ad</sub>". Please unify the symbol and formatting throughout the text and figures, and ensure all units are consistently reported (e.g., mmol/g vs. mmol g<sup>-1</sup>).
6. The sentence "...to finely tune the cation density within the pore cavity to maximize the Xe capture..." could be improved. Consider rephrasing as: "...to modulate cation density and enhance Xe uptake..."
7. In several multi-panel figures (e.g., Figures 2, 3, and 5), panel labels (a–e) are inconsistently placed or not always referenced in the main text. Standardizing these and ensuring all subfigures are cited clearly would improve readability.
8. Some references lack consistent formatting in terms of journal abbreviations, spacing, or superscripts. Please ensure that all references follow the journal's required style.
9. When citing supplementary figures (e.g., "Figure S17 to S22"), it would be beneficial to summarize the relevant findings briefly in the main text to reduce back-and-forth reading.

### Reviewer #3

(Remarks to the Author)

This work reported a strategy of utilizing Ag<sup>+</sup>-exchanged LTA zeolites to achieve the size-inverse molecular sieving for Xe/Kr separation. The authors demonstrate that the exchanged Ag<sup>+</sup> ions within the 8MR create a polarizable gate, which preferentially interact with Xe over Kr despite its larger kinetic diameter. This mechanism is determined by synchrotron PXRD, adsorption isotherms, and DFT calculations, which collectively illustrate how Ag<sup>+</sup> cations serve as dynamic "door-keepers" that selectively admit Xe. Moreover, the incorporation of Ca<sup>2+</sup> ions tunes the cation density and overcomes kinetic limitations, allowing Ag<sub>9</sub>Ca<sub>1.5</sub>A to achieve high dynamic selectivity and Xe uptake. I would like to recommend the acceptance of this manuscript after addressing the following revisions.

- (1) While the authors characterized the presence of Ag<sup>+</sup> ions, long-term stability tests should be applied to determine whether Ag<sup>+</sup> would migration or aggregation.
- (2) The authors identify interaction capacity and size as the key factors in the inverse size mechanism, with computational evidence that the strong interaction between Ag<sup>+</sup> ions and Xe is the main reason for Xe/Kr separation. However, the larger size of Xe is actually unfavorable for the inverse size separation mechanism. Therefore, can the influence of these two factors on the separation results be quantified? If the author could characterize the impact of size on separation, it would make this study more valuable for reference.
- (3) How about the separation performance of these LTA zeolites under humid conditions.
- (4) The authors proposed that the introduction of Ca<sup>2+</sup> ions can address the kinetic limitations in the breakthrough process. How Ca<sup>2+</sup> ions to improve the kinetic performance? It is suggested to clarify.
- (5) The author noted that Ag<sub>9</sub>Ca<sub>1.5</sub>A exhibits improved kinetic performance compared to the pristine Ag<sub>12</sub>A. To further determine this enhanced kinetic performance, the authors are recommended to provide additional breakthrough curves at varying flow rates.

Version 1:

Reviewer comments:

Reviewer #1

(Remarks to the Author)

Reviewer #2

(Remarks to the Author)

I am glad to see that all my previous comments have been carefully addressed. Achieving such highly selective xenon (Xe)/krypton (Kr) separation with industrially important zeolites is both rare and impressive. This work provides valuable insights into a significant breakthrough using traditional materials. The manuscript is now presented with much-improved quality. I have no further comments. Well done, and congratulations to the authors!

Reviewer #3

(Remarks to the Author)

The authors have appropriately addressed the comments by the reviewers. The revised manuscript can be accepted for publication in this journal.

**Open Access** This Peer Review File is licensed under a Creative Commons Attribution 4.0 International License, which permits use, sharing, adaptation, distribution and reproduction in any medium or format, as long as you give appropriate credit to the original author(s) and the source, provide a link to the Creative Commons license, and indicate if changes were made.

In cases where reviewers are anonymous, credit should be given to 'Anonymous Referee' and the source.

The images or other third party material in this Peer Review File are included in the article's Creative Commons license, unless indicated otherwise in a credit line to the material. If material is not included in the article's Creative Commons license and your intended use is not permitted by statutory regulation or exceeds the permitted use, you will need to obtain permission directly from the copyright holder.

To view a copy of this license, visit <https://creativecommons.org/licenses/by/4.0/>

## Response to Reviewers of Manuscript NCOMMS-25-36897-T

The authors wish to express gratitude to the Reviewers for their valuable comments and suggestions regarding our manuscript titled “Size-Inverse Molecular sieving Xenon/Krypton Separation through Cation-Tuned Gating Effect within Linde Type A Zeolites”. We have carefully considered all the Reviewers’ comments and have revised the manuscript to address their concerns. To facilitate the review process, we have provided point-by-point responses to each comment and highlighted all modifications in the manuscript using track changes. We truly appreciate the Reviewers’ time and effort in improving the quality of our work and hope that the revised manuscript meets the high standards required for publication in *Nature Communications*.

Reviewer #1 (Remarks to the Author):

The manuscript entitled “Size-Inverse Molecular Sieving Xenon/Krypton Separation through Cation-Tuned Gating Effect within Linde Type A Zeolites” presents the development of Ag<sup>+</sup> and Ca<sup>2+</sup> ion-exchanged LTA zeolites for Xe/Kr separation via a cation-tuned gating mechanism. The authors report a high IAST selectivity (>1600) for Ag-LTA and a dynamic selectivity of 30 for Ag<sub>9</sub>Ca<sub>1.5</sub>A, supported by adsorption measurements, synchrotron PXRD, XAS, and DFT calculations.

While the technical execution is strong, the manuscript does not meet the novelty and impact criteria for Nature Communications, for the following reasons:

**Response:** We thank the reviewer for the comments and, in particular, for the recognition of the technical execution of the study. With respect to the reviewer’s concerns regarding the novelty and impact of our work, we respectfully wish to provide additional clarification to better highlight the significance of our contribution as follows:

This study represents a fundamental advance in understanding the molecular trapdoor effect. Prior to this work, the molecular trapdoor mechanism for selective gas admission was generally understood to be governed by interactions between guest molecules and the door-keeping cations. In contrast, our findings reveal that *both* the **size** and **interaction capabilities** of *both* the **guest molecules** and **door-keeping cations** act in synergy to regulate selective gas admission. This dual-factor control not only redefines the mechanistic basis of the trapdoor effect but also enables a previously unachievable, counterintuitive outcome: **invertible molecular sieving between Kr and Xe**, whereby either component can be preferentially admitted by rationally tuning the two governing factors.

These mechanistic insights open a new avenue for the design of trapdoor adsorbents and lay the groundwork for advancing high-performance gas separations beyond traditional paradigms, as pointed out by other reviewers as well “This study introduces an invertible molecular sieving mechanism, where selective admission of the larger component (Xe) over the smaller one (Kr) is achieved through an engineered interplay of size and interaction strength rather than conventional size exclusion or

equilibrium affinity alone. By combining adsorption isotherms, in situ synchrotron PXRD, breakthrough experiments, and DFT calculations, we present a comprehensive mechanistic explanation that not only redefines molecular sieving for noble gases but also suggests broader applicability to other challenging separations, such as alkene/alkane mixtures.”

In light of the fundamental novelty, rigorous mechanistic insight, and broader implications of this work, we firmly believe it represents a significant contribution to the field and fully meets the publication criteria for *Nature Communications*.

#### 1. Limited Conceptual Novelty

The cation-tuned gating (or “molecular trapdoor”) effect is well-established in the zeolite literature (e.g., Shang et al., JACS 2012; Lozinska et al., JACS 2012; Zhao et al., JACS 2021). The inversion from Kr-over-Xe to Xe-over-Kr selectivity via Ag<sup>+</sup> exchange, while clearly demonstrated, constitutes a predictable extension of prior work rather than a fundamental advance. Silver-based zeolites for Xe capture have also been previously explored (Daniel et al., J. Phys. Chem. C 2013; Deliere et al., 2014).

**Response:** We sincerely appreciate the reviewer’s acknowledgement that the molecular trapdoor mechanism in zeolites is well-established – a concept originally discovered by some of us (Shang et al., JACS2012) and that this foundational work has since motivated efforts to extend the mechanism to other zeolites and MOFs. We are also grateful for the reviewer’s recognition that our current study clearly demonstrates an inversion in selectivity from Kr-over-Xe to Xe-over-Kr via Ag<sup>+</sup> exchange.

Science advances have been developed step by step. This has been clearly demonstrated in porous materials for gas separations, ranging from traditional zeolites, metal-organic frameworks (MOFs), covalent organic frameworks (COFs) and recently hydrogen bonded organic frameworks (HOFs) in which I am one of the most active researchers on MOFs, COFs and HOFs for gas separations. During our extensive research endeavors in this hot topic, we realized that we still need to develop some unique approaches to target some very challenging gas separations although many strategies have been realized through the pore size fine control, dual/multifunctional pore functions and hierarchical pore engineering for fulfilling high performance gas separations, which has generated many scientific publications in those prestigious journals including *Nature Communications*. For example, the finely tuned pore strategy, a strategy we developed back in 2007 in *Inorganic Chemistry* (“Rationally designed micropores within a metal-organic framework for selective sorption of gas molecules”, *Inorganic Chemistry*, **2007**, *46*, 1233-1236) has been utilized for us to target high-performance gas separation materials in 2016 in *Science* (“Pore chemistry and size control in hybrid porous materials for acetylene capture from ethylene”, *Science*, **2016**, *353* (6295), 141-144) and further developed by other groups as well for gas separations which have been published in many prestigious journals including *Nature Materials*, *Nature Chemistry* and *Nature Communications* recently. Furthermore, the need to reduce the material cost has initiated the community searching for cheaper materials, particularly traditional zeolite materials, to meet such a very important need. You might have already noticed that the cation-tuned gating (or “molecular trapdoor”) effect was discovered back in 2012, but without significant progress over the last decade. This fact, from another perspective, indicates the

very challenge and difficulty of developing such unique porous materials for gas separations. We would also like to respectfully emphasize that this inversion is not a straightforward or predictable extension of prior work. Rather, it represents an **unprecedented and fundamental discovery** that significantly advances the mechanistic understanding of the molecular trapdoor effect, as elaborated in our previous response.

We would like to briefly outline the experimental journey that led to this unexpected finding:

Based on our prior understanding of the molecular trapdoor mechanism, we initially anticipated selective Xe-over-Kr admission in Na-LTA, given Xe's stronger interaction with the Na<sup>+</sup> cation. Surprisingly, experimental results revealed the opposite: **exclusive Kr admission** was observed, indicating that Kr—despite its weaker interaction with Na<sup>+</sup>—could induce the door to open, whereas Xe could not. This suggested that the trapdoor mechanism was not functioning as expected in Na-LTA.

To investigate further, we hypothesized that strengthening the interaction between Xe and the door-keeping cation might restore or enable the molecular trapdoor effect. With this in mind, we selected Ag<sup>+</sup>—a cation known for its strong interaction with Xe—and prepared Ag-LTA as a potential alternative. Remarkably, this substitution **inverted the selectivity**, enabling exclusive Xe admission over Kr.

A detailed analysis of this **invertible molecular sieving**—Kr-over-Xe in Na-LTA and Xe-over-Kr in Ag-LTA—led us to a transformative insight: **both the size and interaction strength of guest molecules and door-keeping cations act synergistically to regulate selective gas admission**. This dual-factor mechanism redefines the foundational understanding of the molecular trapdoor effect and opens new directions for designing advanced trapdoor adsorbents for gas separation.

Regarding the reviewer's concern that silver-based zeolites for Xe capture are not new, we fully acknowledge that prior studies have explored this area (e.g., Daniel *et al.*, *J. Phys. Chem. C*, 2013; Delière *et al.*, *J. Phys. Chem. C*, 2014). However, we would like to clarify that **those studies relied on conventional equilibrium-based adsorption**, where both Xe and Kr have unrestricted access to adsorption sites, and separation was governed by the relatively stronger affinity of Xe, resulting in only modest selectivity. In contrast, our study introduces a **fundamentally different mechanism: size-inverse selective admission governed by the molecular trapdoor effect**, where Ag<sup>+</sup> functions as a door-keeping cation that dynamically regulates gas access. This enables selective gas admission rather than solely relying on equilibrium affinity, thus yielding markedly higher Xe-over-Kr selectivity than previously reported for silver-based systems.

In summary, the findings reported in our work represent a significant discovery and progress in this very important topic, offering both mechanistic innovation and practical implications for gas separation science, and thus have the merits to be published in Nature Communications.

## 2. Discrepancy Between Static and Dynamic Results

Despite the impressive static IAST selectivity, the Ag12A material shows low Xe uptake in dynamic

breakthrough tests, severely limiting practical relevance. While the authors address this by introducing  $\text{Ca}^{2+}$  to enhance sorption kinetics, the dynamic selectivity drops with increased Kr uptake, weakening the claim of “record performance.”

**Response:** Thanks for reviewer’s comments. While IAST selectivity is widely used in the literature, it is well known to often substantially overestimate separation performance. To enable a fair comparison with reported values, we employed IAST selectivity and demonstrated a record-high value in this context. To tackle the kinetic limitations observed in  $\text{Ag}_{12}\text{A}$ , we applied our mechanistic insights into the molecular trapdoor mechanism to rationally design  $\text{AgCa-LTA}$  by incorporating  $\text{Ca}^{2+}$ . This modification achieved a balanced tradeoff between selectivity and adsorption kinetics. Notably, the dynamic selectivity achieved in  $\text{Ag}_9\text{Ca}_{1.5}\text{A}$  represents the highest value reported in the open literature to date (**Figure 5d**).

### 3. Overselling of Impact

Although the mechanism is well supported, the manuscript overstates the breakthrough significance of the work. Known limitations of Ag-zeolites such as silver leaching, long-term stability, and cost, are not adequately discussed or evaluated, which restricts the real-world applicability.

**Response:** We appreciate the reviewer’s thoughtful comment regarding the general concern over the stability of silver-exchanged zeolites, and we fully agree that long-term stability of adsorbents is a critical consideration for real-world applications. We believe that  $\text{Ag}^+$  ions in our silver-exchanged LTA zeolites remain stable for the following reasons. According to the literature, the apparent instability of silver-exchanged zeolites mainly arises at elevated temperatures (approximately 573–773 K), where thermally activated  $\text{Ag}^+$  ion migration leads to Ag aggregation and the formation of Ag clusters (e.g., Grandjean *et al.*, *Science*, 2018). To avoid such degradation, we chose an activation temperature of 473 K prior to adsorption, which is well below the regime associated with cluster formation. In  $\text{Ag-LTA}$  ( $\text{Si/Al} = 1$ ), the framework carries a high density of negative charge and thus strongly requires cationic charge compensation; reducing  $\text{Ag}^+$  to  $\text{Ag}^0$  would result in uncompensated framework charges, thereby energetically disfavoring  $\text{Ag}^+$  degradation. In addition, oxygen atoms at the 8MR and 6MR apertures act as anchoring sites that pin  $\text{Ag}^+$  at specific sites, rendering reduction and aggregation thermodynamically unfavorable under these conditions.

In response to the reviewer’s concern, we have further conducted a comprehensive evaluation of the structural and chemical stability of  $\text{Ag}_{12}\text{A}$ , including potential for silver leaching, using synchrotron PXRD, XAS and XPS. Specifically,  $\text{Ag}_{12}\text{A}$  samples subjected to 10 Xe adsorption-desorption cycles and stored for 1 month were analyzed. Synchrotron PXRD results (**Figures S30 and S31**) confirmed the absence of metallic Ag or  $\text{Ag}_2\text{O}$  phases, and the  $\text{Ag}^+$  sites remained consistent with the pristine material (**Figures S32**). Both XANES (**Figure 3f**) and XPS (**Figure S33**) verified that the oxidation state of Ag remained +1. Furthermore, EXAFS analysis (**Figures 3g and S34; Table S12**) showed no evidence of Ag-Ag bond formation throughout the cycling process. These results collectively demonstrate the excellent long-term structural and chemical stability of  $\text{Ag}_{12}\text{A}$  under the tested conditions. We have included a discussion of these findings in the revised manuscript to address the

reviewer's concern.

Page 6, line 153: Given the common concerns regarding Ag<sup>+</sup> aggregation and leaching in Ag-containing materials,<sup>33-35</sup> we systematically evaluated the long-term stability of Ag<sup>+</sup> in Ag<sub>12</sub>A using synchrotron PXRD, X-ray absorption spectroscopy (XAS), and X-ray photoelectron spectroscopy (XPS). The Ag<sub>12</sub>A sample was subjected to 10 static Xe adsorption-desorption cycles and stored for one month prior to analysis. Synchrotron PXRD patterns showed no evidence of metallic Ag or Ag<sub>2</sub>O formation under 0.1 wt% detection limitation (**Figures S30 and S31**), and Rietveld refinement confirmed that Ag<sup>+</sup> remains stably located at Site I (near the 6MRs) and Site II (at the 8MRs) (**Figure S32**). X-ray absorption near-edge structure (XANES) analysis revealed an absorption edge distinct from that of metallic Ag and Ag<sub>2</sub>O (**Figure 3f**), indicating different coordination environment with the two reference materials. The local environment of Ag<sup>+</sup> within the LTA framework interacts with the zeolite's SiO<sub>4</sub>/AlO<sub>4</sub> network rather than forming typical oxide or metallic bonds. This unique environment alters the electronic structure and shifts the absorption edge. The Ag(3d) XPS measurement further confirmed that Ag<sub>12</sub>A exhibits peak positions (e.g., 3d<sub>5/2</sub> and 3d<sub>3/2</sub>) similar to those of Ag<sub>2</sub>O (**Figure S33**), indicating that silver predominantly exists in the monovalent state. In addition, extended X-ray absorption fine structure (EXAFS) spectra showed a prominent peak at approximately 1.8 Å (**Figure 3g**), corresponding to Ag<sup>+</sup>-framework oxygen coordination, with negligible Ag-Ag contributions, excluding the possibility of silver clustering. Quantitative fitting of the Ag K-edge EXAFS spectra showed precise Ag-O bond lengths of 2.25 Å and 2.38 Å (**Figure S34 and Table S12**), corresponding to 6MR and 8MR oxygen atoms, respectively. These results collectively demonstrate the excellent chemical and structural stability of Ag<sup>+</sup> in Ag<sub>12</sub>A, with no evidence of leaching or aggregation under the tested conditions.

We understand the reviewer's concern regarding the cost of Ag-containing zeolites. It is worth noting that among the noble metals, Ag is relatively low in cost, making it a more economically viable choice. We further estimated the cost of synthesizing Ag<sub>12</sub>A based on the method reported in this work. 2 g of zeolite 4A (Sigma Aldrich, priced at \$77.40 for 500 g, or \$0.155/g) were ion exchanged in 50 mL of 0.2 M silver nitrate solution (silver nitrate powder, Sigma Aldrich, priced at \$1825.90 for 500 g, or \$3.65/g), yielding 3.2 g of Ag<sub>12</sub>A. Thus, the material synthesis cost is approximately \$2/g. It is important to note that the 0.2 M silver nitrate concentration was chosen to ensure complete Ag<sup>+</sup> exchange in zeolite 4A; further analysis indicated that a concentration of about 0.1 M would achieve nearly 100% Ag<sup>+</sup> exchange, reaching **a cost of Ag<sub>12</sub>A around \$1.07/g**. In contrast, other MOF and COF materials with good performance for Xe/Kr separation typically **cost between \$10 and \$50/g**, significantly higher than Ag<sub>12</sub>A in this work. Furthermore, as demonstrated above, the Ag-LTA adsorbents exhibit excellent long-term stability. Given their relatively low cost and high durability, the use of Ag is unlikely to impose a significant economic burden on practical applications.

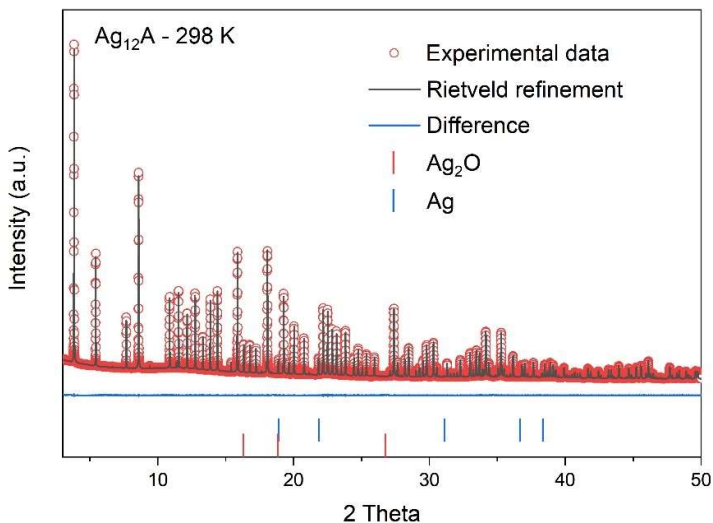


Figure S30. Fitted Synchrotron PXRD profiles of dehydrated  $\text{Ag}_{12}\text{A}$  at 298 K, overlaid with the characteristic peaks of  $\text{Ag}_2\text{O}$  and  $\text{Ag}$  for comparison. Prior to measurement, the sample underwent 10 cycles of Xe adsorption-desorption, was stored for one month, and thermally activated at 473 K for 8 hours.

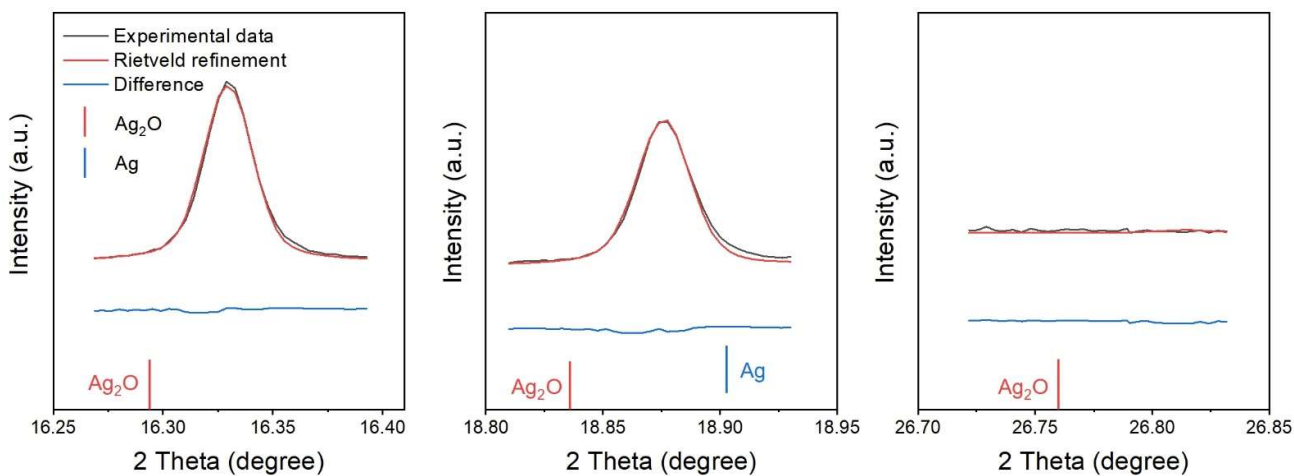


Figure S31. Enlarged synchrotron PXRD patterns of Figure S30 showing no characteristic peaks corresponding to  $\text{Ag}_2\text{O}$  or  $\text{Ag}$ .

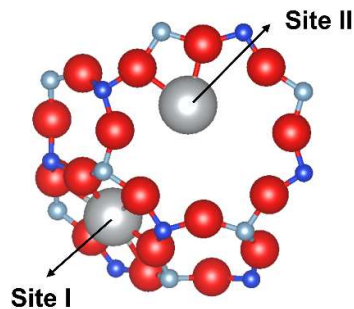


Figure S32. The crystal structure of dehydrated  $\text{Ag}_{12}\text{A}$  with  $\text{Ag}^+$  sites, resolved from synchrotron

PXRD patterns by Rietveld refinement: Ag (grey), Si (deep blue), Al (light blue), O (red). Prior to measurement, the sample underwent 10 cycles of Xe adsorption-desorption, was stored for one month, and thermally activated at 473 K for 8 hours.

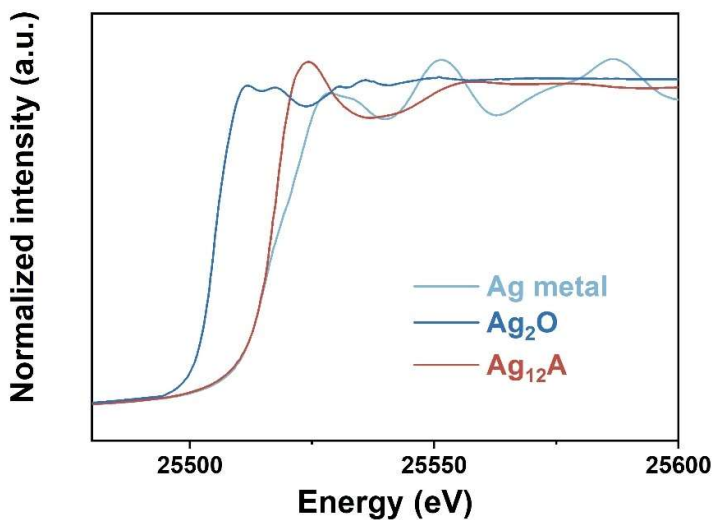


Figure 3(f). XANES spectra of dehydrated Ag<sub>12</sub>A at 298 K, shown alongside reference spectra of Ag metal and Ag<sub>2</sub>O. Prior to measurement, the sample underwent 10 cycles of Xe adsorption-desorption, was stored for one month, and thermally activated at 473 K for 8 hours.

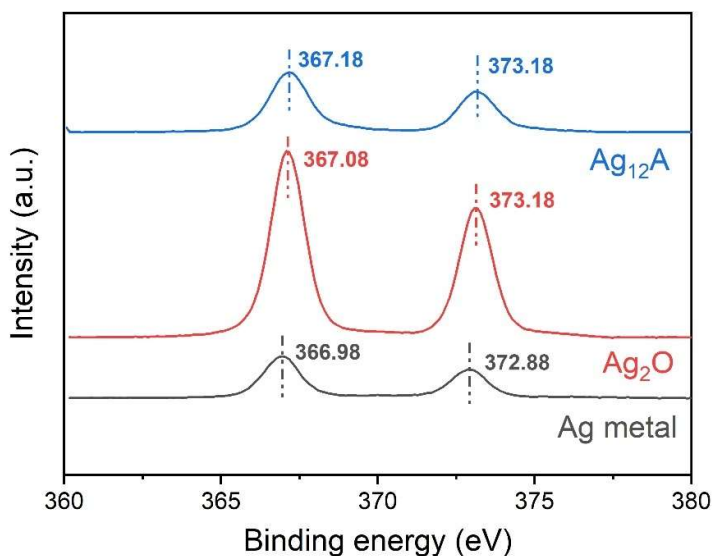


Figure S33. Ag(3d) XPS spectra of Ag metal, Ag<sub>2</sub>O, and Ag<sub>12</sub>A after 10 Xe adsorption-desorption cycles and 1-month storing. The 3d<sub>5/2</sub> (367.18 eV) and 3d<sub>3/2</sub> (373.18 eV) binding energies of Ag<sub>12</sub>A indicate that Ag predominantly exists in the monovalent state.

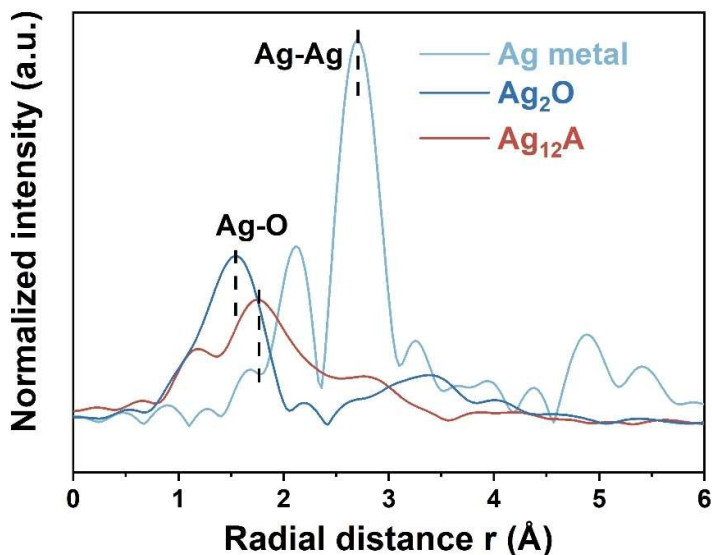


Figure 3(g). Fourier transforms of EXAFS spectra of dehydrated  $\text{Ag}_{12}\text{A}$  at 298 K, shown alongside reference spectra of Ag metal and  $\text{Ag}_2\text{O}$ . Prior to measurement, the sample underwent 10 cycles of Xe adsorption-desorption, was stored for one month, and thermally activated at 473 K for 8 hours.

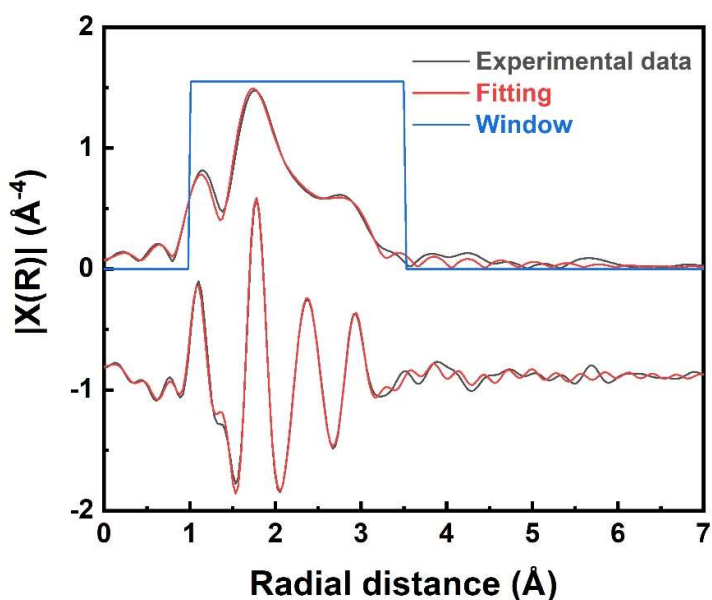


Figure S34. EXAFS fitting curves at Ag K-edge of dehydrated  $\text{Ag}_{12}\text{A}$  at 298 K. Prior to measurement, the sample underwent 10 cycles of Xe adsorption-desorption, was stored for one month, and thermally activated at 473 K for 8 hours.

Table S12. Fitting parameters obtained from EXAFS analysis at Ag K-edge of dehydrated  $\text{Ag}_{12}\text{A}$  at 298 K. R is the interatomic distance, N is the coordination number,  $\sigma^2$  is the Debye-Waller factor, and  $\Delta E_0$  is the threshold energy shift. R-factor represents the goodness-of-fit.

Path	R (Å)	N	$\sigma^2$ (Å <sup>2</sup> )	$\Delta E_0$ (eV)	R-factor (%)
------	-------	---	------------------------------	-------------------	--------------

<b>Ag-O1</b>	<b>2.25(1)</b>	<b>3.0(1)</b>	<b>0.006(1)</b>	<b>2.1(2)</b>	<b>1.1%</b>
<b>Ag-O2</b>	<b>2.37(3)</b>	<b>2.1(1)</b>	<b>0.009(2)</b>	<b>2.1(2)</b>	<b>1.1%</b>
<b>Ag-Al/Si</b>	<b>2.85(3)</b>	<b>4.0(1)</b>	<b>0.009(2)</b>	<b>2.1(2)</b>	<b>1.1%</b>

#### 4. Incremental Improvement Over Prior Work

The tuning of cation density and mixed-cation strategies for gas separation are well-known techniques. The authors present a refined system, but not one that introduces a new material class or separation mechanism. The work thus falls short of the broader conceptual advances expected by Nature Communications.

In conclusion, this manuscript is well executed and presents a compelling mechanistic study of cation-gated Xe/Kr separation in LTA zeolites. However, the work represents an incremental advance rather than a transformative contribution, and the key claims are weakened by performance limitations under realistic conditions. Given these concerns, I do not recommend publication in Nature Communications. The manuscript may be better suited for a specialized journal in adsorption or materials chemistry.

**Response:** We appreciate the reviewer's critical assessment and acknowledge that our explanation of the novelty and broader significance of this work could have been more clearly articulated. While it is true that tuning cation density and employing mixed-cation strategies have been previously explored in gas separation, we respectfully submit that our study introduces a **previously unreported and conceptually significant advancement** in both the mechanistic understanding and application of the molecular trapdoor effect. Specifically, this work contributes in the following key ways:

##### 1. **Clarification of the role of cation tuning within a distinct separation mechanism:**

We acknowledge that **cation density tuning and mixed-cation strategies are well-known techniques** in equilibrium-based adsorptive separations, where cations function primarily as **static adsorption sites** that determine selectivity via differential binding affinities. In contrast, our work focuses on a **molecular trapdoor-controlled system**, where cations play a **dual role**: not only do they serve as adsorption sites, but more importantly, they act as **dynamic door-keepers** that regulate the energy barrier for gas admission. Tuning cation identity and distribution in this context **modulates the accessibility of guest molecules** to the internal framework by adjusting the energetic threshold required for passage, enabling a fundamentally different and more selective mode of separation.

##### 2. **New mechanistic insight into selective gas admission:**

We establish and experimentally validate a mechanistic framework based on the **synergistic interplay between molecular size and interaction strength of both guest molecules and door-keeping cations**, governing gas admission through the trapdoor effect. This dual-factor regulation departs from traditional views and reveals an additional layer of kinetic control not captured in previous studies.

3. **Reversible, size-inverse molecular sieving:**

We demonstrate a **previously unobserved, reversible inversion of selectivity**—from Kr-over-Xe in Na-LTA to Xe-over-Kr in Ag-LTA—achieved solely by substituting the door-keeping cation. This **invertible molecular sieving effect**, driven by dynamic gas admission rather than static affinity or size exclusion, represents a fundamental advance in the design of responsive adsorbents.

4. **First demonstration of trapdoor-based Xe/Kr separation:**

This is the **first report of using the molecular trapdoor mechanism for Xe-selective adsorption**, achieving dynamic Xe-over-Kr selectivity that **surpasses all known Xe-selective materials**. Current systems relying on equilibrium adsorption suffer from limited selectivity, while conventional molecular sieving and kinetic separation favor Kr, leading to suboptimal performance. Our approach offers a superior selectivity-capacity balance through **selective admission control**.

5. **Mechanistically grounded and generalizable design principle:**

The ability to manipulate cation identity to tune the kinetic accessibility of guest molecules offers a **generalizable strategy** for designing high-performance adsorbents. The principles established here may be extended to other demanding separations, such as alkene/alkane or polar/non-polar mixtures, where selective gatekeeping could provide unique advantages.

In summary, while this study builds upon prior knowledge, it **goes beyond incremental refinement**. It redefines the role of cation tuning by establishing a mechanism in which **selective gas admission is governed by the synergistic interplay between molecular size and interaction strength—of both the guest molecules and the door-keeping cations**. This leads to a **new and reversible molecular sieving paradigm**, and introduces a **high-performing Xe-selective system** that operates through **gas admission control rather than conventional affinity-based adsorption**. We believe these contributions constitute a **substantial conceptual advance** and align well with the expectations of *Nature Communications*.

Reviewer #2 (Remarks to the Author):

The manuscript titled “Size-Inverse Molecular Sieving Xenon/Krypton Separation through Cation-Tuned Gating Effect within Linde Type A Zeolites” presents a compelling conceptual and experimental advance in gas separation science. The authors develop a new paradigm for Xe/Kr separation using a cation-tuned gating mechanism in Linde Type A (LTA) zeolites, achieving a remarkable IAST selectivity of over 1600 and dynamic selectivity of 30. This is enabled by the selective interaction between Xe and  $\text{Ag}^+$  cations at key pore sites and is further optimized via partial substitution with  $\text{Ca}^{2+}$  to alleviate kinetic limitations.

This work stands out for introducing an invertible molecular sieving mechanism, where the selective admission of the larger component (Xe) over the smaller one (Kr) is achieved through engineered gas-cation interactions rather than conventional size exclusion or equilibrium affinity alone. The authors combine adsorption isotherms, in situ synchrotron PXRD, breakthrough experiments, and DFT calculations to provide a thorough mechanistic explanation. Their approach not only redefines molecular sieving for noble gases but also suggests broader applicability to other challenging separations such as alkene/alkane mixtures.

Given the fundamental novelty, practical relevance, and excellent experimental and theoretical rigor, this is an outstanding and highly impactful piece of work. I strongly recommend minor revision prior to acceptance. The following comments are intended solely to clarify and strengthen the presentation, and do not detract from the scientific quality or significance of the findings. I look forward to seeing this work published following revision.

We sincerely thank the reviewer for the very positive overall comments and the strong recommendation for publication. We are also grateful for the valuable and insightful suggestions, which have significantly improved the quality of our revised manuscript. All identified errors and inaccuracies have been carefully addressed, with detailed responses provided to each comment below.

Some specific questions and suggestions for the authors' consideration:

1. The manuscript states that  $\text{Ag}^+$  and  $\text{Ca}^{2+}$  cannot be distinguished via diffraction in AgCa-LTA materials. However, it remains unclear which cation is primarily occupying the 8MR sites and acting as the door-keeping species. Since this directly affects the gating behavior, the authors should elaborate on any experimental trends (e.g., from synchrotron PXRD, EXAFS) or simulations (e.g., relative adsorption energies or stabilities) that may support a cation-specific site preference or functional role. Even a semi-quantitative trend would strengthen the mechanistic interpretation.

**Response:** Thanks for the comments. We apologize for the lack of clarity in explaining the site preference of mixed  $\text{Ag}^+$  and  $\text{Ca}^{2+}$  in LTA zeolites. As noted, synchrotron PXRD alone cannot unambiguously distinguish  $\text{Ag}^+$  from  $\text{Ca}^{2+}$  because Rietveld refinement returns electron density rather than elemental identity. We have now performed further analysis of those PXRD data, in combination with new DFT calculations and XAS data to determine the cation site preference in AgCa-LTA.

Using  $\text{Ag}_{10}\text{Ca}_1\text{A}$  as an example, the refined electron density at the 8MR site is identical to that of

Ag<sub>12</sub>A (**Figure S57; Table S16**), indicating that the 8MR remains fully occupied by Ag<sup>+</sup>. Any Ca<sup>2+</sup> substitution at the 8MR site would lower the local electron density due to its scattering factor. By contrast, the 6MR site electron density decreases to 94% of that in Ag<sub>12</sub>A (**Figure S57; Table S16**), which we attribute to (1) the reduced total cation number upon introducing divalent Ca<sup>2+</sup>, leaving some 6MR sites vacant, and (2) partial substitution of Ag<sup>+</sup> by Ca<sup>2+</sup> at 6MR sites.

The DFT calculations have now been performed to examine the site preference of Ca<sup>2+</sup>, which indicated that Ca<sup>2+</sup> preferentially occupies 6MR sites over 8MR sites, with an energy difference of 0.84 eV (**Table S18**). This finding agrees well with XRD results, where Ca<sup>2+</sup> prefers 6MRs over 8MRs in Ag<sub>10</sub>Ca<sub>1</sub>A. Consistently, Ca K-edge XAS gives an average Ca–O distance of 2.38 Å (**Figures S58 to S60; Table S19**), reasonably close to the DFT-predicted Ca–O distances at 6MR (2.29–2.31 Å) and 8MR (2.26–2.28 Å) (**Figure S61**), supporting the reliability of the DFT structural models.

Overall, the combined PXRD, DFT, and XAS evidence indicates that Ca<sup>2+</sup> resides preferentially at 6MR in AgCa-LTA, whereas the 8MR apertures remain occupied by door-keeping Ag<sup>+</sup> cations.

For clarity, the revisions have been added to the manuscript and the SI as detailed below.

Page 10, line 277: To determine cation site preference after Ca<sup>2+</sup> incorporation, synchrotron PXRD tests were conducted on a series of dehydrated AgCa-LTA zeolites (**Figures S54 to S56; Table S16**). By analyzing changes in electron density at different cation sites and considering charge balance, specific cation site preferences can be determined. Using Ag<sub>10</sub>Ca<sub>1</sub>A as an illustrative example, the refined electron density at the 8MR site is identical to that of Ag<sub>12</sub>A (**Figure 57; Table S16**), indicating that 8MR remains fully occupied by Ag<sup>+</sup>. Any Ca<sup>2+</sup> substitution would reduce the local electron density due to its lower scattering factor. In contrast, the electron density at the 6MR site decreases to 94% of that in Ag<sub>12</sub>A (**Figure S57; Table S16**), attributed to (1) reduced total cation numbers from introducing divalent Ca<sup>2+</sup>, and (2) partial substitution of Ag<sup>+</sup> by Ca<sup>2+</sup> at the 6MRs.

DFT calculations confirm that Ca<sup>2+</sup> preferentially occupies 6MR sites over 8MR sites, with an energy difference of 0.84 eV (**Table S18**), consistent with the 6MR site preference of Ca<sup>2+</sup> observed in XRD results. Furthermore, Ca K edge XAS gives an average Ca–O distance of 2.38 Å (**Figures S58 to S60; Table S19**), reasonably close to the DFT predicted Ca–O distances at 6MR (2.29–2.31 Å) and 8MR (2.26–2.28 Å) (**Figure S61**), supporting the reliability of the DFT structural models.

Overall, the combined PXRD, DFT, and XAS evidence indicates that Ca<sup>2+</sup> resides preferentially at 6MR in AgCa-LTA, whereas Ag<sup>+</sup> still occupies the 8MR site, acting as door-keeping cation.

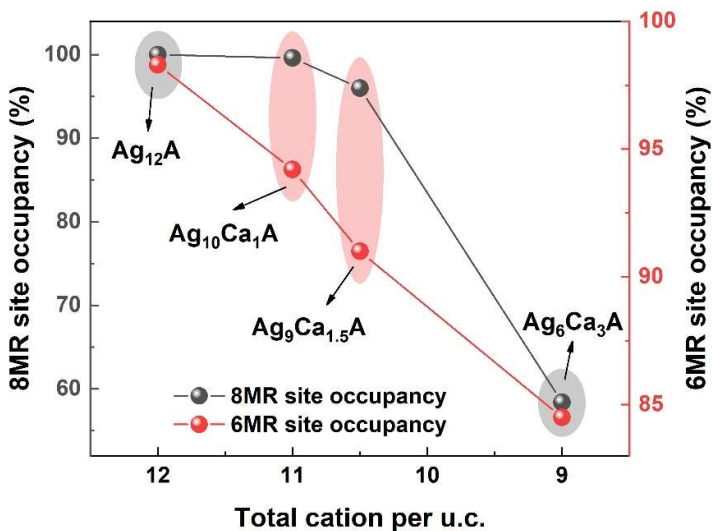


Figure S57. Site I (6MR) and Site II (8MR) occupancy change in dehydrated AgCa-LTA zeolites at 298 K. All cations are assumed as Ag<sup>+</sup> for the ease of presentation.

Table S18. Summary of the calculated relative energies of Ca<sup>2+</sup> at Site I (6MR) and Site II (8MR) in LTA zeolites. Cation energy at Site II is set to 0 eV. Ca<sup>2+</sup> exhibits a preference for Site I over Site II.

Cation type	Relative Energy (eV)	
	8MR site	6MR site
Ca <sup>2+</sup>	0	-0.84

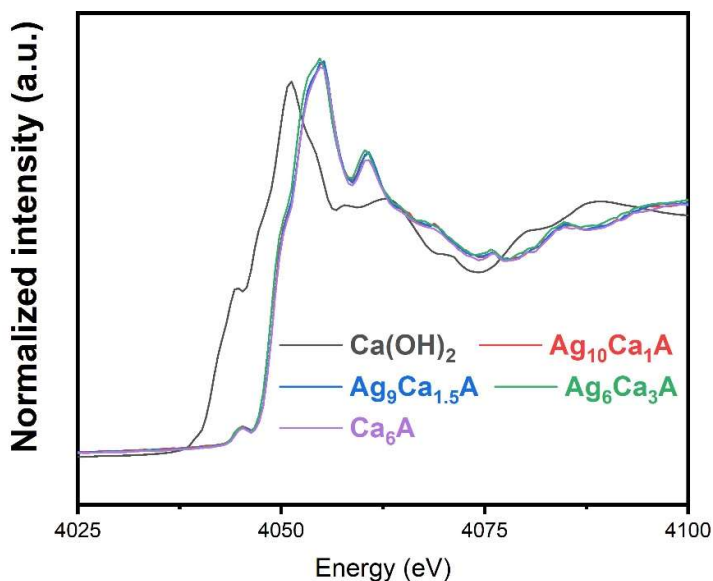


Figure S58. XANES spectra for dehydrated AgCa-LTA zeolites at 298 K, shown alongside reference spectra of Ca(OH)<sub>2</sub>. Prior to measurement, the samples were thermally activated at 473 K for 8 hours.

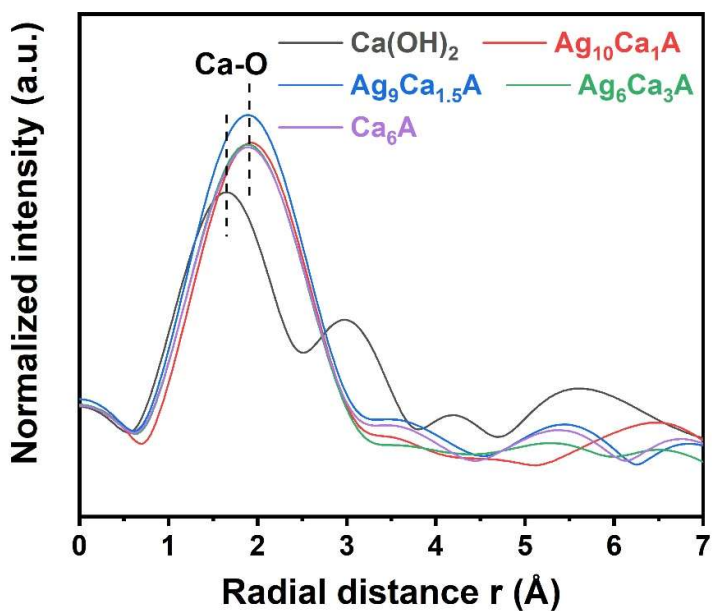


Figure S59. Fourier transforms of EXAFS spectra of dehydrated AgCa-LTA zeolites at 298 K, shown alongside reference spectra of  $\text{Ca}(\text{OH})_2$ . Prior to measurement, the samples were thermally activated at 473 K for 8 hours.

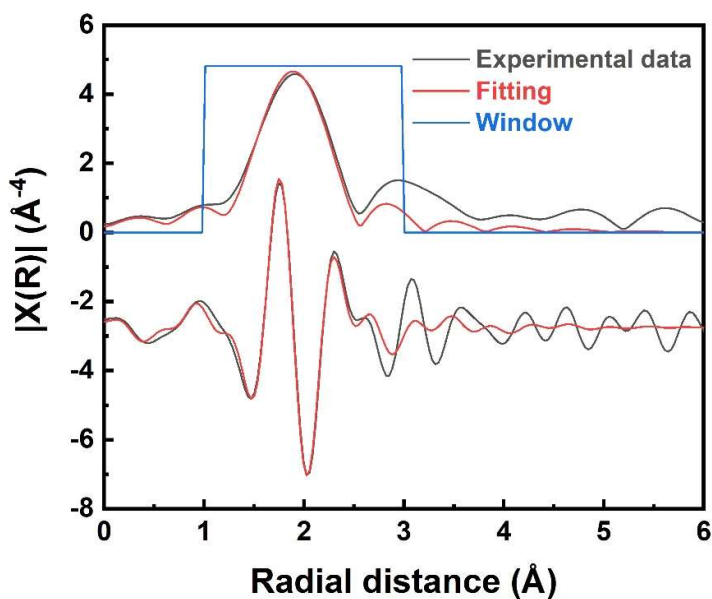
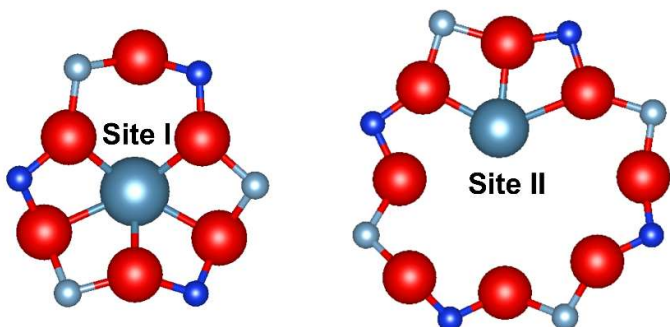


Figure S60. EXAFS fitting curves at Ca K-edge of dehydrated  $\text{Ag}_9\text{Ca}_{1.5}\text{A}$  at 298 K. Prior to measurement, the samples were thermally activated at 473 K for 8 hours.

Table S19. Fitting parameters obtained from EXAFS analysis at Ca K-edge of dehydrated  $\text{Ag}_9\text{Ca}_{1.5}\text{A}$  at 298 K. R is the interatomic distance, N is the coordination number,  $\sigma^2$  is the Debye-Waller factor, and  $\Delta E_0$  is the threshold energy shift. R-factor represents the goodness-of-fit.

Path	R (Å)	N	$\sigma^2$ (Å <sup>2</sup> )	$\Delta E_o$ (eV)	R-factor (%)
Ca-O1	2.38 (3)	3.3(1)	0.007(1)	3.7(2)	1.6



Ca-O distance = 2.30 Å

Ca-O distance = 2.27 Å

Figure S61. The crystal structures and Ca-O distance at Site I (6MR) and Site II (8MR) in LTA scaffold, derived from DFT calculations: Si (deep blue), Al (light blue), O (red), Ca (light blue).

2. While the performance of Ag-LTA is impressive, several small-pore zeolites (e.g., CHA, KFI) are also known to exhibit molecular trapdoor effects. The authors should briefly justify the selection of LTA over other candidates. Is the framework geometry, cation accessibility, exchangeability, or known industrial usage the primary reason? A concise rationale would clarify the generalizability of this strategy.

**Response:** Thanks for the comments. Indeed, several other small-pore zeolites have been reported to exhibit the molecular trapdoor effect. Here, we selected the LTA scaffold for the following two reasons:

1. To study Na<sup>+</sup> and Ag<sup>+</sup> as door-keeping cations for regulating selective gas admission through the molecular trapdoor mechanism, it is crucial that all 8MR apertures in the zeolite frameworks are fully occupied by the target cations. LTA zeolite (Si/Al = 1) naturally fulfills this requirement, as the unique cation site distribution in both Na-LTA and Ag-LTA ensures complete occupation of the 8MR apertures. In contrast, other small-pore zeolites like CHA, typically synthesized with higher Si/Al ratios (2-3), exhibit cation site preferences and distributions that prevent full cation occupation of the 8MR apertures, making them unsuitable for investigating Na<sup>+</sup> and Ag<sup>+</sup> as effective door-keeping cations.
2. LTA is one of the most well-known zeolites, in academic research and industrial applications. Showcasing the selective separation of Xe and Kr through the molecular trapdoor mechanism in LTA would not only promote the broader dissemination of these findings but also increase their potential for practical implementation.

For clarity, the sentence has been added to the manuscript below.

Page 3, line 83: To study  $\text{Na}^+$  and  $\text{Ag}^+$  as door-keeping cations for regulating selective gas admission through the cation-tuned gating effect, it is essential that all 8MR apertures in small-pore zeolites are fully occupied by the target cations. LTA zeolite ( $\text{Si}/\text{Al} = 1$ ) is particularly suited for this purpose due to its unique cation site distribution and occupancy. Structurally, LTA zeolite features a body-centered cubic arrangement of LTA and sodalite (SOD) cages, with 8MRs ( $4.1 \times 4.1 \text{ \AA}$ ) serving as the only access for guest molecules to the supercavities. Three distinct sites exist within the framework: site I (located at 6MRs), site II (at 8MRs) and site III (at 4MRs) as shown in **Figure 1b**.<sup>30</sup> Among these sites,  $\text{Na}^+$  and  $\text{Ag}^+$  at site II typically residing in the plane of 8MRs play a critical role in regulating gas accessibility, rendering LTA a suitable scaffold for developing  $\text{Na}^+$ - and  $\text{Ag}^+$ -based cation-tuned gating adsorbents.

3. The authors state that  $\text{Ag}_6\text{Ca}_3\text{A}$  shows measurable  $\text{N}_2$  uptake and BET surface area, implying a loss of cation-induced gating. Could the authors provide further insight into why the trapdoor mechanism collapses in this sample? Does  $\text{Ca}^{2+}$  incorporation exceed a critical threshold that weakens cation-framework interactions, displaces cations from 8MRs, or otherwise disrupts the gating configuration?

**Response:** Thanks for the comments. To ensure the molecular trapdoor effect operates effectively, a very high degree of 8MR blockage (close to 100%) is required (*J. Phys. Chem. C*, 2013, 117(24), 12841-12847). As revealed by the resolved synchrotron PXRD in **Figure S57**, the reduced cation density in  $\text{Ag}_6\text{Ca}_3\text{A}$ , due to the partial exchange monovalent  $\text{Ag}^+$  with divalent  $\text{Ca}^{2+}$ , significantly lowers the percentage of 8MR blockage to approximately 60%. Consequently, the trapdoor effect is lost, or “collapsed”, allowing  $\text{N}_2$  admission at 77 K. This is reflected by measurable  $\text{N}_2$  uptake at this temperature and a corresponding increase in BET surface area. For clarity, we have revised the manuscript as shown below.

Page 11, line 293: Based on the resolved synchrotron PXRD results (**Figure S57; Table S16**), the  $\text{Ag}^+$  occupancy at the 8MR sites was quantified as follows: 99.7% for  $\text{Ag}_{10}\text{Ca}_1\text{A}$ , 96.0% for  $\text{Ag}_9\text{Ca}_{1.5}\text{A}$ , and 58.6% for  $\text{Ag}_6\text{Ca}_3\text{A}$ . The near-complete occupancy of the 8MR sites in the first two materials aligns with their negligible  $\text{N}_2$  uptake at 77 K (**Figure S52; Table S15**). In contrast, the significant incorporation of  $\text{Ca}^{2+}$  in  $\text{Ag}_6\text{Ca}_3\text{A}$  drastically reduces the density of door-keeping  $\text{Ag}^+$ , effectively negating the trapdoor effect. As a result,  $\text{N}_2$  molecules gain access at 77 K, leading to measurable  $\text{N}_2$  uptake and a corresponding increase in BET surface area (**Figure S52; Table S15**).

4. The manuscript introduces the term “size-inverse sieving” to describe preferential adsorption of the larger component (Xe). As this terminology may be unfamiliar to general readers, a clear definition early in the abstract or introduction would be helpful.

**Response:** Thanks for the reviewer’s suggestions. Accordingly, we have revised the introduction part with a definition of the term “size-inverse molecular sieving”.

Page 2, line 71: .....meaning that larger Xe can be exclusively admitted and adsorbed while smaller Kr is excluded for admission and adsorption.

5. The manuscript refers to the threshold admission temperature using notations like “T\_ad” or “Tad”. Please unify the symbol and formatting throughout the text and figures, and ensure all units are consistently reported (e.g., mmol/g vs. mmol g<sup>-1</sup>).

**Response:** Thanks for the reviewer’s suggestions. We have updated the notations for the threshold admission temperature to  $T_c$  throughout the text and figures. Additionally, we have verified the consistency of all units used.

6. The sentence “...to finely tune the cation density within the pore cavity to maximize the Xe capture...” could be improved. Consider rephrasing as: “...to modulate cation density and enhance Xe uptake...”.

**Response:** Thanks for the reviewer’s correction. The sentence has been revised accordingly.

Page 1, line 25: Through the cation exchange by Ag<sup>+</sup> to introduce the preferential binding of Xe over Kr gas, followed by Ca<sup>2+</sup> exchange to modulate cation density within the pore cavity so as to facilitate Xe uptake, the resulting Ag<sub>9</sub>Ca<sub>1.5</sub>A overcomes the kinetic limitations and achieves a dynamic Xe/Kr selectivity of 30 — the highest reported in the open literature — along with a high dynamic Xe uptake of 1.65 mmol/g.

7. In several multi-panel figures (e.g., Figures 2, 3, and 5), panel labels (a–e) are inconsistently placed or not always referenced in the main text. Standardizing these and ensuring all subfigures are cited clearly would improve readability.

**Response:** Thanks for the suggestions. We have standardized the placement of panel labels across all multi-panel figures including Figure 2, 3, and 5 to ensure consistency. Additionally, we have carefully reviewed the main text to ensure all subfigures are clearly cited and properly referenced.

8. Some references lack consistent formatting in terms of journal abbreviations, spacing, or superscripts. Please ensure that all references follow the journal’s required style.

**Response:** Thanks for bringing this to our attention. We have thoroughly checked all references and made revisions where necessary to ensure consistent formatting, including journal abbreviations, spacing, and superscripts, in accordance with the journal’s style.

9. When citing supplementary figures (e.g., “Figure S17 to S22”), it would be beneficial to summarize the relevant findings briefly in the main text to reduce back-and-forth reading.

**Response:** Thanks for the reviewer’s suggestion. To help minimize back-and-forth reading and improve the flow of information, we have revised the main text to ensure the correspondence in the isobar analysis of Ag<sub>5</sub>Na<sub>7</sub>A and Ag<sub>12</sub>A.

Page 4, line 121: Isobar analyses of  $\text{Ag}_5\text{Na}_7\text{A}$  (Figures S17 to S20) and  $\text{Ag}_{12}\text{A}$  (Figure 2c, Figures S21 and S22) further indicate that  $\text{Ag}^+$  incorporation remarkably lower  $T_c(\text{Xe})$  while raising  $T_c(\text{Kr})$  relative to  $\text{Na}_{12}\text{A}$ .

Reviewer #3 (Remarks to the Author):

This work reported a strategy of utilizing Ag<sup>+</sup>-exchanged LTA zeolites to achieve the size-inverse molecular sieving for Xe/Kr separation. The authors demonstrate that the exchanged Ag<sup>+</sup> ions within the 8MR create a polarizable gate, which preferentially interact with Xe over Kr despite its larger kinetic diameter. This mechanism is determined by synchrotron PXRD, adsorption isotherms, and DFT calculations, which collectively illustrate how Ag<sup>+</sup> cations serve as dynamic “door-keepers” that selectively admit Xe. Moreover, the incorporation of Ca<sup>2+</sup> ions tunes the cation density and overcomes kinetic limitations, allowing Ag<sub>9</sub>Ca<sub>1.5</sub>A to achieve high dynamic selectivity and Xe uptake. I would like to recommend the acceptance of this manuscript after addressing the following revisions.

Thank you for your invaluable and constructive comments, which have greatly contributed to enhancing the quality of this work.

(1) While the authors characterized the presence of Ag<sup>+</sup> ions, long-term stability tests should be applied to determine whether Ag<sup>+</sup> would migration or aggregation.

**Response:** Thanks for the reviewer’s comments and we agree that this is a valid concern. We understand that long-term stability is crucial for practical applications, especially for silver-exchanged zeolites that may suffer from leaching or aggregation. We believe that Ag<sup>+</sup> ions in our silver-exchanged LTA zeolites remain stable for the following reasons. According to the literature, the apparent instability of silver-exchanged zeolites mainly arises at elevated temperatures (approximately 573–773 K), where thermally activated Ag<sup>+</sup> ion migration leads to Ag aggregation and the formation of Ag clusters (e.g., Grandjean *et al.*, *Science*, 2018). To avoid such degradation, we chose an activation temperature of 473 K prior to adsorption, which is well below the regime associated with cluster formation. In Ag–LTA (Si/Al = 1), the framework carries a high density of negative charge and thus strongly requires cationic charge compensation; reducing Ag<sup>+</sup> to Ag<sup>0</sup> would result in uncompensated framework charges, thereby energetically disfavoring Ag<sup>+</sup> degradation. In addition, oxygen atoms at the 8MR and 6MR apertures act as anchoring sites that pin Ag<sup>+</sup> at specific sites, rendering reduction and aggregation thermodynamically unfavorable under these conditions.

In response to the reviewer’s concern, we have further conducted a comprehensive evaluation of the structural and chemical stability of Ag<sub>12</sub>A, including potential for silver leaching, using synchrotron PXRD, XAS and XPS. Specifically, Ag<sub>12</sub>A samples subjected to 10 Xe adsorption-desorption cycles and stored for 1 month were analyzed. Synchrotron PXRD results (**Figures S30 and S31**) confirmed the absence of metallic Ag or Ag<sub>2</sub>O phases, and the Ag<sup>+</sup> sites remained consistent with the pristine material (**Figures S32**). Both XANES (**Figure 3f**) and XPS (**Figure S33**) verified that the oxidation state of Ag remained +1. Furthermore, EXAFS analysis (**Figures 3g and S34; Table S12**) showed no evidence of Ag-Ag bond formation throughout the cycling process. These results collectively demonstrate the excellent long-term structural and chemical stability of Ag<sub>12</sub>A under the tested conditions. We have included a discussion of these findings in the revised manuscript to address the reviewer’s concern.

Page 6, line 153: Given the common concerns regarding  $\text{Ag}^+$  aggregation and leaching in  $\text{Ag}$ -containing materials,<sup>33-35</sup> we systematically evaluated the long-term stability of  $\text{Ag}^+$  in  $\text{Ag}_{12}\text{A}$  using synchrotron PXRD, X-ray absorption spectroscopy (XAS), and X-ray photoelectron spectroscopy (XPS). The  $\text{Ag}_{12}\text{A}$  sample was subjected to 10 static Xe adsorption-desorption cycles and stored for one month prior to analysis. Synchrotron PXRD patterns showed no evidence of metallic  $\text{Ag}$  or  $\text{Ag}_2\text{O}$  formation under 0.1 wt% detection limitation (**Figures S30 and S31**), and Rietveld refinement confirmed that  $\text{Ag}^+$  remains stably located at Site I (near the 6MRs) and Site II (at the 8MRs) (**Figure S32**). X-ray absorption near-edge structure (XANES) analysis revealed an absorption edge distinct from that of metallic  $\text{Ag}$  and  $\text{Ag}_2\text{O}$  (**Figure 3f**), indicating different coordination environment with the two reference materials. The local environment of  $\text{Ag}^+$  within the LTA framework interacts with the zeolite's  $\text{SiO}_4/\text{AlO}_4$  network rather than forming typical oxide or metallic bonds. This unique environment alters the electronic structure and shifts the absorption edge. The  $\text{Ag}(3d)$  XPS measurement further confirmed that  $\text{Ag}_{12}\text{A}$  exhibits peak positions (e.g.,  $3d_{5/2}$  and  $3d_{3/2}$ ) similar to those of  $\text{Ag}_2\text{O}$  (**Figure S33**), indicating that silver predominantly exists in the monovalent state. In addition, extended X-ray absorption fine structure (EXAFS) spectra showed a prominent peak at approximately 1.8 Å (**Figure 3g**), corresponding to  $\text{Ag}^+$ -framework oxygen coordination, with negligible  $\text{Ag}$ - $\text{Ag}$  contributions, excluding the possibility of silver clustering. Quantitative fitting of the  $\text{Ag}$   $K$ -edge EXAFS spectra showed precise  $\text{Ag}$ - $\text{O}$  bond lengths of 2.25 Å and 2.38 Å (**Figure S34 and Table S12**), corresponding to 6MR and 8MR oxygen atoms, respectively. These results collectively demonstrate the excellent chemical and structural stability of  $\text{Ag}^+$  in  $\text{Ag}_{12}\text{A}$ , with no evidence of leaching or aggregation under the tested conditions.

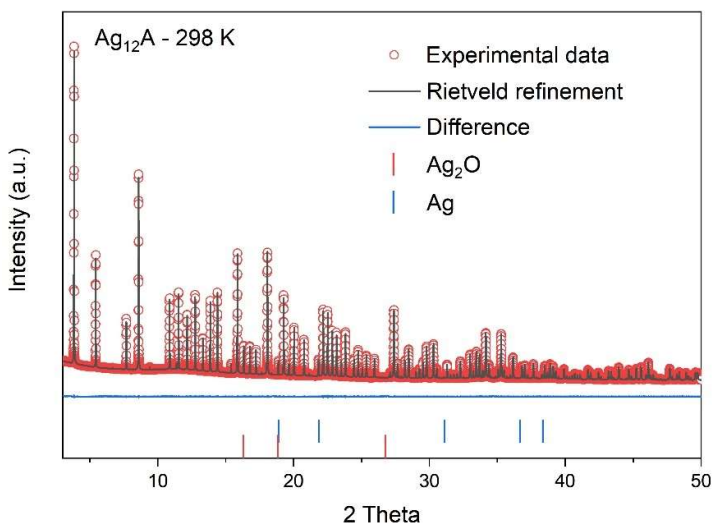


Figure S30. Fitted Synchrotron PXRD profiles of dehydrated  $\text{Ag}_{12}\text{A}$  at 298 K, overlaid with the characteristic peaks of  $\text{Ag}_2\text{O}$  and  $\text{Ag}$  for comparison. Prior to measurement, the sample underwent 10 cycles of Xe adsorption-desorption, was stored for one month, and thermally activated at 473 K for 8 hours.

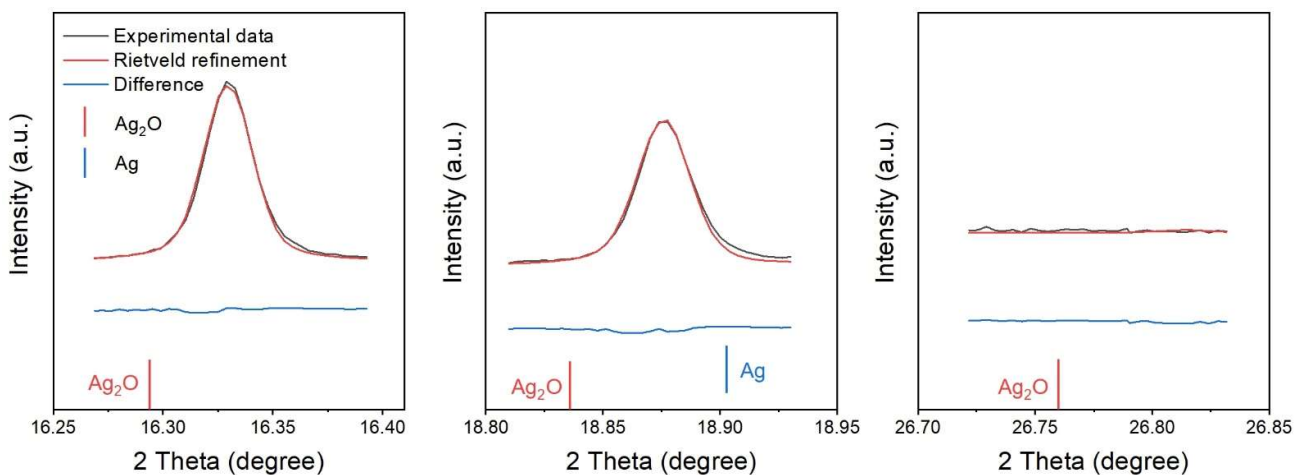


Figure S31. Enlarged synchrotron PXRD patterns of Figure S30 showing no characteristic peaks corresponding to  $\text{Ag}_2\text{O}$  or  $\text{Ag}$ .

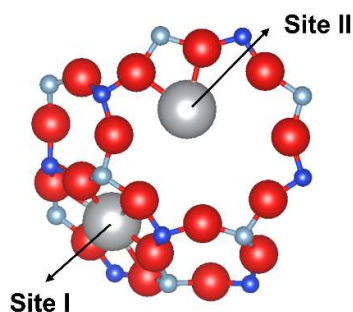


Figure S32. The crystal structure of dehydrated  $\text{Ag}_{12}\text{A}$  with  $\text{Ag}^+$  sites, resolved from synchrotron PXRD patterns by Rietveld refinement:  $\text{Ag}$  (grey),  $\text{Si}$  (deep blue),  $\text{Al}$  (light blue),  $\text{O}$  (red). Prior to measurement, the sample underwent 10 cycles of  $\text{Xe}$  adsorption-desorption, was stored for one month, and thermally activated at 473 K for 8 hours.

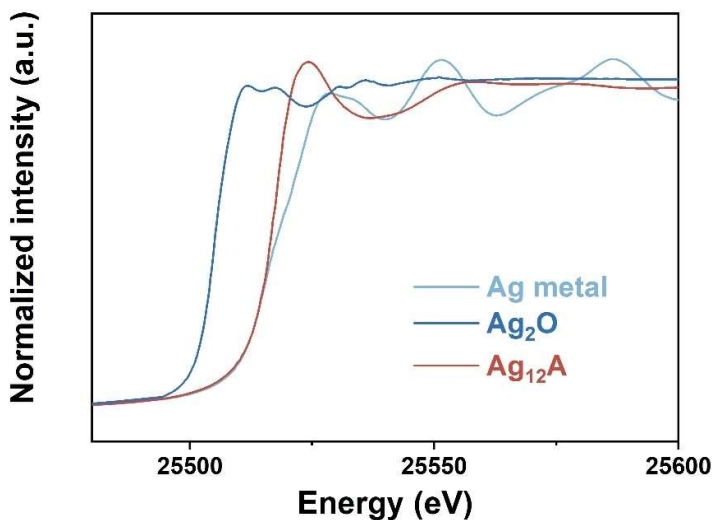


Figure 3(f). XANES spectra of dehydrated  $\text{Ag}_{12}\text{A}$  at 298 K, shown alongside reference spectra of  $\text{Ag}$

metal and  $\text{Ag}_2\text{O}$ . Prior to measurement, the sample underwent 10 cycles of Xe adsorption-desorption, was stored for one month, and thermally activated at 473 K for 8 hours.

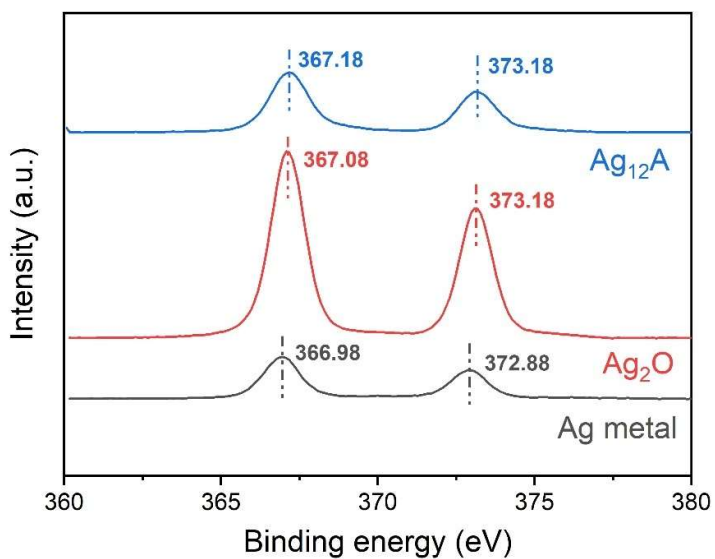


Figure S33.  $\text{Ag}(3d)$  XPS spectra of Ag metal,  $\text{Ag}_2\text{O}$ , and  $\text{Ag}_{12}\text{A}$  after 10 Xe adsorption-desorption cycles and 1-month storing. The  $3d_{5/2}$  (367.18 eV) and  $3d_{3/2}$  (373.18 eV) binding energies of  $\text{Ag}_{12}\text{A}$  indicate that Ag predominantly exists in the monovalent state.

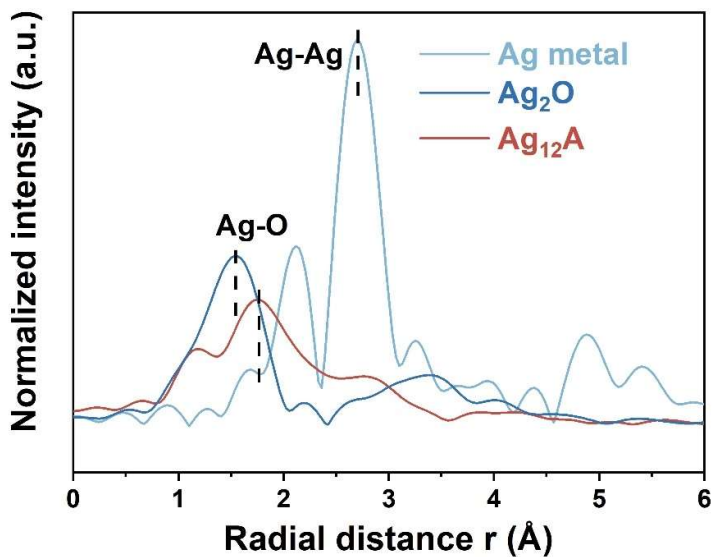


Figure 3(g). Fourier transforms of EXAFS spectra of dehydrated  $\text{Ag}_{12}\text{A}$  at 298 K, shown alongside reference spectra of Ag metal and  $\text{Ag}_2\text{O}$ . Prior to measurement, the sample underwent 10 cycles of Xe adsorption-desorption, was stored for one month, and thermally activated at 473 K for 8 hours.

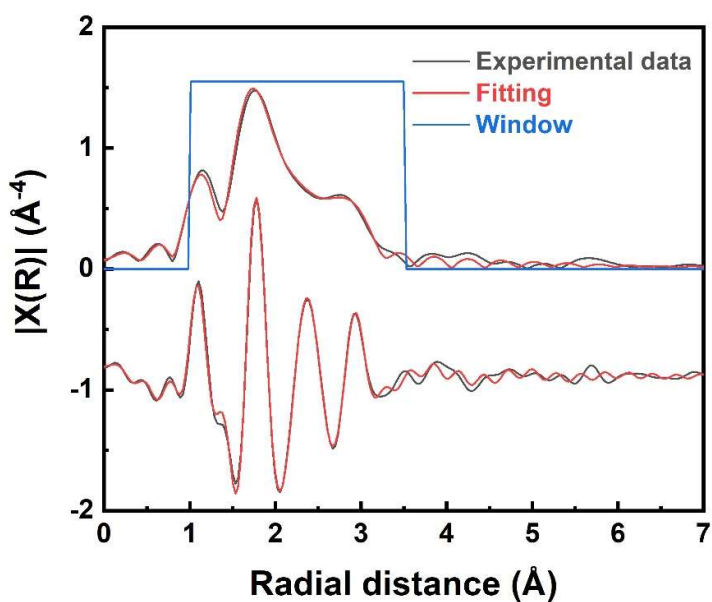


Figure S34. EXAFS fitting curves at Ag K-edge of dehydrated  $\text{Ag}_{12}\text{A}$  at 298 K. Prior to measurement, the sample underwent 10 cycles of Xe adsorption-desorption, was stored for one month, and thermally activated at 473 K for 8 hours.

Table S12. Fitting parameters obtained from EXAFS analysis at Ag K-edge of dehydrated  $\text{Ag}_{12}\text{A}$  at 298 K. R is the interatomic distance, N is the coordination number,  $\sigma^2$  is the Debye-Waller factor, and  $\Delta E_0$  is the threshold energy shift. R-factor represents the goodness-of-fit.

Path	R (Å)	N	$\sigma^2$ (Å <sup>2</sup> )	$\Delta E_o$ (eV)	R-factor (%)
Ag-O1	2.25(1)	3.0(1)	0.006(1)	2.1(2)	1.1%
Ag-O2	2.37(3)	2.1(1)	0.009(2)	2.1(2)	1.1%
Ag-Al/Si	2.85(3)	4.0(1)	0.009(2)	2.1(2)	1.1%

(2) The authors identify interaction capacity and size as the key factors in the inverse size mechanism, with computational evidence that the strong interaction between Ag<sup>+</sup> ions and Xe is the main reason for Xe/Kr separation. However, the larger size of Xe is actually unfavorable for the inverse size separation mechanism. Therefore, can the influence of these two factors on the separation results be quantified? If the author could characterize the impact of size on separation, it would make this study more valuable for reference.

**Response:** Thanks for the constructive suggestions. We acknowledge that in the process of Xe/Kr separation, the two factors of size and interaction are correlated and can potentially be quantified. At this stage, a rigorous quantitative decoupling of size and interaction effects remains challenging due to the limited number of gas species studied. However, we agree that this is an important direction for future work. To enable a more systematic analysis, we plan to expand our investigation to include a broader set of monoatomic gases (e.g., He, Ne, Ar) and inert diatomic gases (e.g., N<sub>2</sub>, O<sub>2</sub>), which span a range of sizes and polarizabilities. This would allow us to better disentangle the relative contributions of steric and energetic factors to gas admission. We also recognize that additional molecular descriptors—such as adsorption configuration, polarizability, dipole and quadrupole moments, and the electronic structure of the door-keeping cations—must be considered to capture the full complexity of the trapdoor mechanism. We are currently exploring these directions and appreciate the reviewer’s encouragement to deepen the analysis in this regard.

(3) How about the separation performance of these LTA zeolites under humid conditions.

**Response:** Thank you for the reviewer’s insightful comment. We agree that accounting for moisture is crucial for practical adsorbent applications. Zeolites with high aluminum content are inherently hydrophilic, and their performance is often compromised under humid conditions due to competitive water adsorption. Water molecules strongly interact with both the framework and extraframework cations, reducing adsorption capacity and selectivity. Molecular trapdoor zeolites, with their high cation density, are similarly vulnerable. We acknowledge this limitation and recognize the need to develop trapdoor systems with greater humidity tolerance for real-world use. At this stage, the standard mitigation strategy is to pre-dry the Xe/Kr gas stream prior to adsorption.

(4) The authors proposed that the introduction of Ca<sup>2+</sup> ions can address the kinetic limitations in the

breakthrough process. How Ca<sup>2+</sup> ions to improve the kinetic performance? It is suggested to clarify.

**Response:** Thanks for the reviewer's question regarding the role of Ca<sup>2+</sup> incorporation in Ag-LTA and its impact on adsorption kinetics. We believe the enhanced adsorption kinetics primarily arise from two aspects: (1) the reduced cation density at Site I near the 6MRs, which alleviates the difficulty of moving the door-keeping cations at adjacent 8MR sites, thereby lowering the energy barrier of the door-opening process; and (2) the decreased density of door-keeping Ag<sup>+</sup> cations at 8MRs, which reduces the number of events in which gas molecules must overcome the energy barrier to get admitted and adsorbed. Both reducing the magnitude of the energy barrier for door-opening and decreasing the number of events of restricted admission are expected to enhance the adsorption kinetics. We have now performed further analysis of those PXRD data to determine the role of Ca<sup>2+</sup> incorporation in adsorption kinetics.

Taking Ag<sub>9</sub>Ca<sub>1.5</sub>A as an example, the refined electron density at the 6MR site is measured at only 91% of that observed in Ag<sub>12</sub>A (**Figure S57; Table S16**). The reduction arises from two factors: (1) partial substitution of Ag<sup>+</sup> by Ca<sup>2+</sup>, as Ag<sup>+</sup> has a higher electron density than Ca<sup>2+</sup>, and (2) the creation of vacant cation sites associated with this substitution. Based on the charge balance, cation site preference, and cation electron density, Ca<sup>2+</sup> occupies 18.8% of the 6MR sites, leaving 5% of these sites vacant. In our original submission, DFT calculations predicted that, with fully occupied 6MR sites, the only viable route for door-keeping cation movement was a perpendicular shift from the 8MR towards the gas side (**Figure S41**). The 5% vacant 6MR sites provide an alternative route, allowing door-keeping cation movement towards the 6MR, which is expected to significantly alleviate the difficulty of door-keeping cation displacement, lowers the energy barrier for door-opening, and enhances adsorption kinetics.

Additionally, the electron density at the 8MR in Ag<sub>9</sub>Ca<sub>1.5</sub>A decreases to 96% compared to that of Ag<sub>12</sub>A (**Figure S57; Table S16**), indicating a 4% reduction in door-keeping Ag<sup>+</sup> cations, thereby creating 4% vacant 8MR sites. This directly reduces the number of events in which gas molecules must overcome the energy barrier for adsorption, further improving adsorption kinetics.

The revisions have been incorporated into the manuscript as detailed below.

Page 10, line 259: To address this limitation, we proposed incorporating divalent cations into Ag<sub>12</sub>A. Specifically, Ca<sup>2+</sup> was selected as the representative divalent cation, as it is among the most common in LTA frameworks (e.g., zeolite 5A). Divalent cations are expected to reduce the number of extraframework cations required to balance the charge of the zeolite framework, thereby creating vacant cation sites. Considering the site distribution of Ag<sup>+</sup> and Ca<sup>2+</sup>, we hypothesize that these vacant cation sites may appear at either Site II on the 8MRs or Site I near the 6MRs, both of which could enhance sorption kinetics because: (1) Reducing the density of door-keeping cations at the 8MRs decreases the number of events for cation deviation; (2) Reducing the density of non-door-keeping cations at the 6MRs would alleviate repulsive cation-cation interactions and lower the energy barrier for cation deviation.

Page 11, line 310: To investigate how Ca<sup>2+</sup> incorporation enhanced adsorption kinetics, we further

analyzed the cation site occupancy using synchrotron PXRD of AgCa-LTA. Taking  $\text{Ag}_9\text{Ca}_{1.5}\text{A}$  as a representative example, the refined electron density at the 6MR site is only 91% of that observed in  $\text{Ag}_{12}\text{A}$  (Figure S57; Table S16). Based on charge balance, cation site preference, and electron density, it is determined that  $\text{Ca}^{2+}$  occupies 18.8% of the 6MR sites, leaving 5% of these sites vacant. Note that in  $\text{Ag}_{12}\text{A}$  with fully occupied 6MR sites, DFT calculations predicted that the only viable route for the movement of door-keeping cations was a perpendicular shift from the 8MR towards the gas side (Figure S41). The presence of 5% vacant 6MR sites introduces an alternative pathway, allowing door-keeping movement towards the 6MR. This would reduce the difficulty of door-keeping cation displacement, lower the energy barrier for door-opening, and thereby enhance adsorption kinetics.

Furthermore, the electron density at the 8MR site in  $\text{Ag}_9\text{Ca}_{1.5}\text{A}$  decreases to 96% of that in  $\text{Ag}_{12}\text{A}$  (Figure S57; Table S16), indicating a 4% reduction in door-keeping  $\text{Ag}^+$  cations with 4% vacant 8MR sites. This directly reduces the number of events in which gas molecules must overcome the energy barrier for admission and adsorption, thus improving adsorption kinetics.

Therefore, the enhanced adsorption kinetics after  $\text{Ca}^{2+}$  incorporation primarily arise from two aspects: (1) the reduced cation density of non-door-keeping cations near the 6MRs, which alleviates the difficulty of moving the door-keeping cations at adjacent 8MR sites, thereby lowering the energy barrier of the door-opening process; and (2) the decreased density of door-keeping cations at 8MRs, which reduces the number of events for cation deviation.

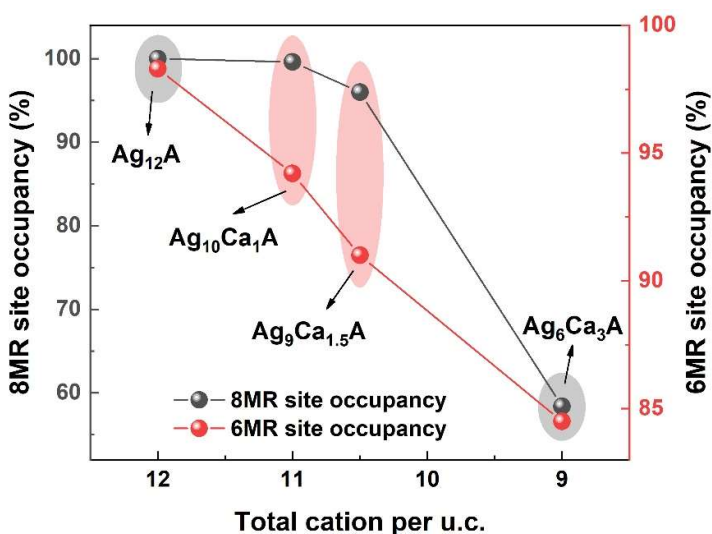


Figure S57. Site I (6MR) and Site II (8MR) occupancy change in dehydrated AgCa-LTA zeolites at 298 K. All cations are assumed as  $\text{Ag}^+$  for the ease of presentation.

(5) The author noted that  $\text{Ag}_9\text{Ca}_{1.5}\text{A}$  exhibits improved kinetic performance compared to the pristine  $\text{Ag}_{12}\text{A}$ . To further determine this enhanced kinetic performance, the authors are recommended to provide additional breakthrough curves at varying flow rates.

**Response:** Thanks for the suggestions. It is indeed necessary to measure breakthrough curves at varying flow rates on Ag<sub>12</sub>A and Ag<sub>9</sub>Ca<sub>1.5</sub>A to show the enhanced kinetic performance. In our original submission, a total flow rate of 10 cc/min was used with a Xe/Kr component ratio of 20/80, using Ar as the carrier gas. To further illustrate the enhanced kinetic performance, we conducted additional experiments at total flow rates of 15 cc/min and 20 cc/min on both samples while maintaining the same component ratio.

The results show that Ag<sub>9</sub>Ca<sub>1.5</sub>A retains excellent Xe/Kr separation performance even at higher total flow rates. The high dynamic Xe uptake and Xe/Kr selectivity of Ag<sub>9</sub>Ca<sub>1.5</sub>A remain uncompromised (**Figures S78 and S79**), indicating fast adsorption kinetics. In contrast, Ag<sub>12</sub>A with sluggish adsorption kinetics continues to exhibit negligible uptake for both Xe and Kr at higher total flow rates (**Figures S80 and S81**). We have incorporated these results into the manuscript and the SI.

Page 12, line 334: The high dynamic Xe uptake and selectivity of Ag<sub>9</sub>Ca<sub>1.5</sub>A are not compromised when the flow rate is increased (**Figures S78 and S79**), further corroborating the markedly enhanced adsorption kinetics relative to Ag<sub>12</sub>A (**Figures S80 and S81**).

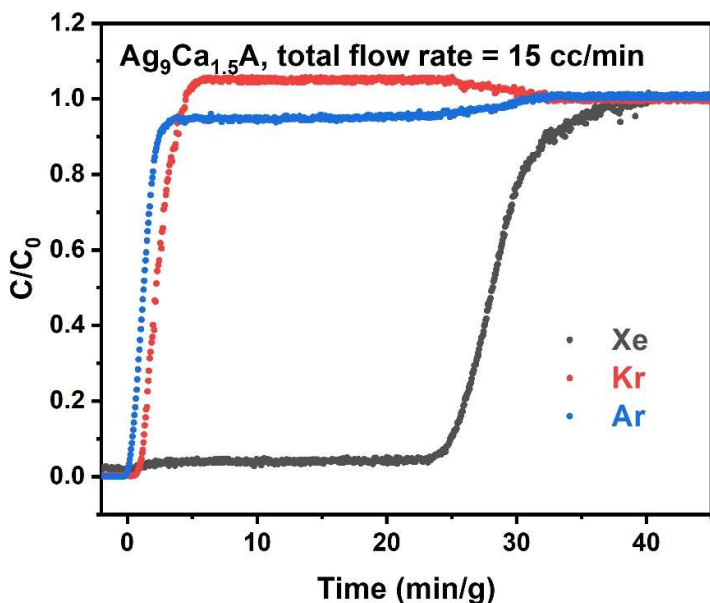


Figure S78. Dynamic gas breakthrough curve of the Xe/Kr = 20/80 using Ar as a carrier gas on Ag<sub>9</sub>Ca<sub>1.5</sub>A at 298 K and 1 bar. Total gas flow rate= 15 cc/min (Xe 1.5 cc/min, Kr 6 cc/min, Ar 7.5 cc/min).

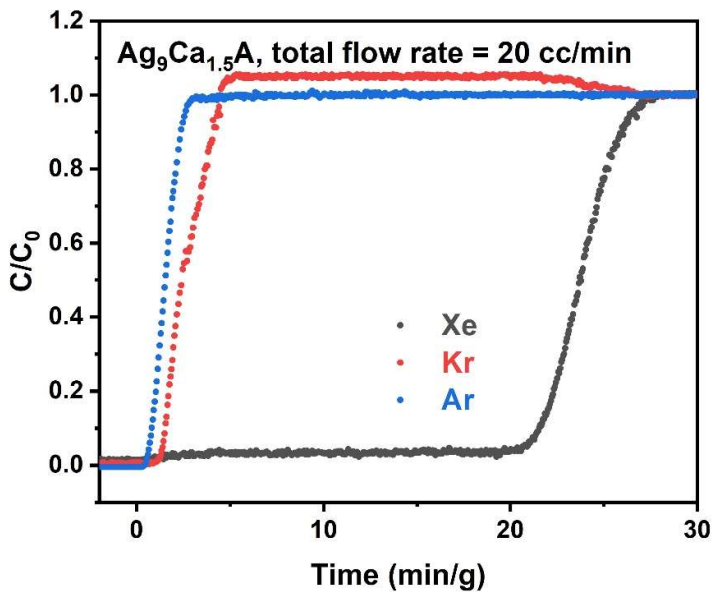


Figure S79. Dynamic gas breakthrough curve of the Xe/Kr = 20/80 using Ar as a carrier gas on  $\text{Ag}_9\text{Ca}_{1.5}\text{A}$  at 298 K and 1 bar. Total gas flow rate = 20 cc/min (Xe 2 cc/min, Kr 8 cc/min, Ar 10 cc/min).

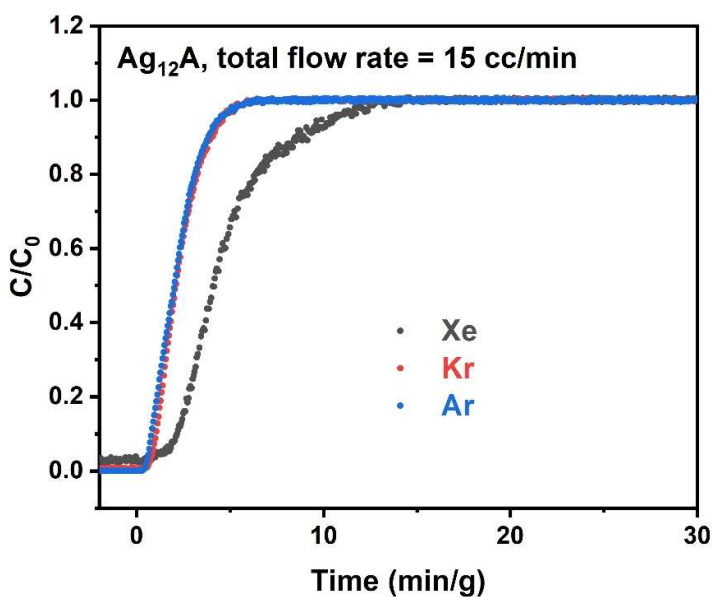


Figure S80. Dynamic gas breakthrough curve of the Xe/Kr = 20/80 using Ar as a carrier gas on  $\text{Ag}_{12}\text{A}$  at 298 K and 1 bar. Total gas flow rate = 15 cc/min (Xe 1.5 cc/min, Kr 6 cc/min, Ar 7.5 cc/min).

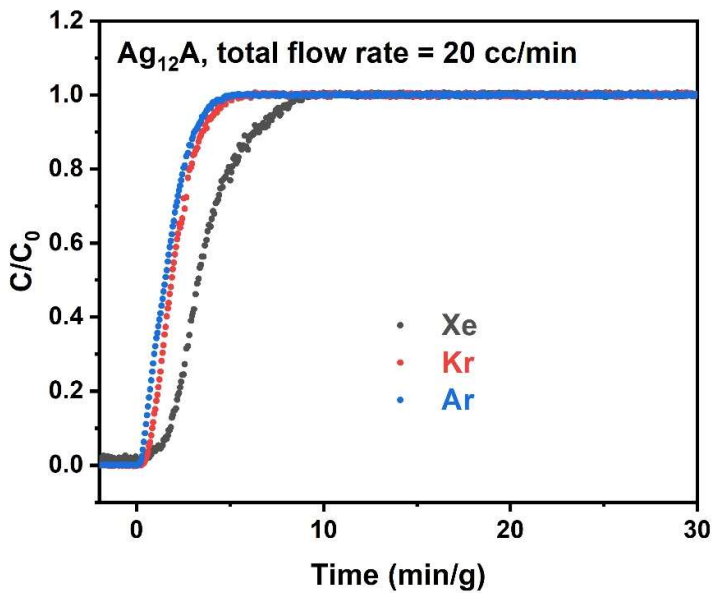


Figure S81. Dynamic gas breakthrough curve of the Xe/Kr = 20/80 using Ar as a carrier gas on Ag<sub>12</sub>A at 298 K and 1 bar. Total gas flow rate = 20 cc/min (Xe 2 cc/min, Kr 8 cc/min, Ar 10 cc/min).